Erschienen in: Neurobiology of Aging ; 34 (2013), 1. - S. 184-199
https://dx.doi.org/10.1016/j.neurobiolaging.2012.03.012

Control of Aβ release from human neurons by differentiation status and RET signaling

Diana Scholz *, Yana Chernyshova, Marcel Leist

Department of Biology, University of Konstanz, Konstanz, Germany

Abstract

Few studies have compared the processing of endogenous human amyloid precursor protein (APP) in younger and older neurons. Here, we characterized LUHMES cells as a human model to study Alzheimer's disease-related processes during neuronal maturation and aging. Differentiated LUHMES expressed and spontaneously processed APP via the secretase pathways, and they secreted amyloid β (Aβ) peptide. This was inhibited by cholesterol depletion or secretase inhibition, but not by block of tau phosphorylation. In vitro aged cells increased Aβ secretion without upregulation of APP or secretases. We identified the medium constituent glial cell line-derived neurotrophic factor (GDNF) as responsible for this effect. GDNF-triggered Aβ release was associated with rapid upregulation of the GDNF coreceptor "rearranged during transfection" (RET). Other direct (neurturin) or indirect (nerve growth factor) RET activators also increased Aβ, whereas different neurotrophins were ineffective. Downstream of RET, we found activation of protein kinase B (AKT) to be involved. Accordingly, inhibitors of the AKT regulator phosphatidylinositol-3-kinase completely blocked GDNF-triggered AKT phosphorylation and Aβ increase. This suggests that RET signaling affects Aβ release from aging neurons.

Keywords: LUHMES; Alzheimer's disease; Aβ; RET; GDNF

1. Introduction

Amyloid precursor protein (APP) is abundantly expressed in neurons and can be proteolytically processed by several secretases. The soluble extracellular peptide sAPPα is released by α-secretase. Alternative cleavage by β-secretase (BACE) releases a slightly smaller soluble N-terminal fragment (sAPPβ). The γ-secretase complex is able to process the remaining membrane-bound C-terminal fragments. Sequential β- and γ-secretase cleavage generates the amyloid β peptide (Aβ), which is prone to aggregate and to form the plaques that are a hallmark of Alzheimer's disease (AD) (Zhang et al., 2011). Aβ levels have been found to increase with age in human brains (Fukumoto et al., 1996) and APP transgenic mouse lines (Hsiao et al., 1996). Thus, age-related cellular changes that affect the pathways of Aβ generation or clearance are regarded as major factors in the etiology of AD. The causes for these changes are still largely unknown. The same holds true for the formation of intracellular neurofibrillary tangles, the second hallmark of AD. Their main component is the hyperphosphorylated form of the microtubule-associated protein tau. The interaction of phosphorylated tau and Aβ may accelerate the progressive neurodegeneration in the course of AD (Ballatore et al., 2007; Ittner and Götz, 2011).

Glial cell line-derived neurotrophic factor (GDNF) and its congeners neurturin (NRTN), artemin, and persephin comprise the group of neurotrophic GDNF family ligands (GFLs) (Airaksinen and Saarma, 2002). GFLs signal through their cognate receptors, consisting of a GDNF family receptor α subunit (GFRα1–4) as ligand binding component specific for each member, and the "rearranged during transfection" (RET) receptor tyrosine kinase as common signaling component (Takahashi, 2001). RET activation can also be elicited by nerve growth factor (NGF), probably due

* Corresponding author at: University of Konstanz, Universitätsstraße 10, Postbox M657, D-78457 Konstanz, Germany. Tel.: +49 7531 885136; fax: +49 7531 885039.

E-mail address: diana.scholz@gmx.net (D. Scholz).

to a crosstalk between neurotrophic tyrosine kinase receptor type 1 (TrkA) and RET (Tsui-Pierchala et al., 2002). RET targets several downstream signaling cascades, such as the mitogen-activated protein kinase (MAPK), phosphatidylinositol-3-kinase (PI3K), phospholipase Cγ (PLCγ) and Src kinase pathways (Manié et al., 2001; Wells and Santoro, 2009).

In contrast to the role of GDNF-triggered RET signaling in neuronal survival and differentiation (Airaksinen and Saarma, 2002), its effect on the production of Aβ has not been well examined due to the lack of model systems. Other receptor tyrosine kinases such as those stimulated by NGF or brain-derived neurotrophic factor (BDNF), have been more easily accessible and are known to modulate Aβ generation (Adlerz et al., 2007; Gianni et al., 2003; Matrone et al., 2008a; Zou et al., 2007).

LUHMES cells are conditionally immortalized human neuronal precursor cells (Lotharius et al., 2002). Upon inactivation of the *v-myc* transgene expression by tetracycline, they differentiate into a homogeneous population of irreversibly postmitotic and electrically active neurons within 5 days (Scholz et al., 2011). Besides their general neuronal characteristics, such as the formation of an extensive neurite network (Stiegler et al., 2011), the cells show features of dopaminergic neurons (Lotharius et al., 2005; Schildknecht et al., 2009), including RET expression and responsiveness to GDNF. So far, investigations regarding proteins relevant for Alzheimer's disease in LUHMES cells have been neglected, although nigral neurodegeneration and the presence of Aβ plaques in the striatum of AD brains have been well documented by several groups (Kalaitzakis et al., 2008; Uchihara et al., 1992; Villemagne et al., 2009). This indicates that substantia nigra neurons are indeed able to secrete pathologic Aβ (Cai et al., 2010) and could play a so far underestimated role in AD, for example by seeding plaques through the terminals of their projections as has been proposed for brainstem neurons (Muresan and Muresan, 2008).

We initiated this study to investigate the expression and processing of AD-relevant proteins in LUHMES cells. Our findings suggest that differentiated LUHMES provide the opportunity to examine changes of endogenous human tau and APP within the same cell. Moreover, they allow the study of effects of the neuronal maturation status and of neurotrophic factor signaling, such as the GDNF-RET system, on APP processing.

2. Methods

2.1. Chemicals

Wortmannin, LY294002, rapamycin, phorbol 12,13-dibutyrate (PDBu), methyl-β-cyclodextrin (MβCD), and simvastatin were obtained from Sigma-Aldrich (St. Louis, MO, USA). Simvastatin was dissolved in ethanol and turned into the activated acid form by treatment with NaOH prior to use (Sadeghi et al., 2000). Bisindolylmaleimide 1 (Bis1), SU6656, U0126, the indolinone-based RET receptor tyrosine kinase inhibitor RPI-1 (Cuccuru et al., 2004), and okadaic acid as well as the BACE inhibitor "isophtalamide derivative" (IPAD, sold as beta-secretase inhibitor IV) (Stachel et al., 2004; Volbracht et al., 2009), OM99-2, and N-[N-(3,5-di-fluorophenacetyl)-L-alanyl]-S-phenylglycine t-butyl ester (DAPT) were purchased from Merck (Darmstadt, Germany). CHIR98014 and PIK-90 were from Axon Instruments Medchem (Groningen, The Netherlands). LY450139 and the BACE inhibitor "aminoquinazoline derivative" (AQD, originally named BACE inhibitor 3a) (Baxter et al., 2007) were synthesized following the schemes provided by Lilly (Indianapolis, IN, USA).

2.2. Cell culture

LUHMES were grown and differentiated at 37 °C in a humidified 95% air/5% CO_2 atmosphere as described previously (Schildknecht et al., 2009; Scholz et al., 2011). In brief, Nunclon plastic lab ware (Nunc, Roskilde, Denmark) or glass cover slips (Menzel, Braunschweig, Germany) were precoated for 3 hours with poly-L-ornithine/fibronectin (Sigma-Aldrich) in H_2O. Cells were plated after enzymatic dissociation with advanced trypsin versene (ATV) solution (138 mM NaCl, 5.4 mM KCl, 6.9 mM $NaHCO_3$, 5.6 mM D-glucose, 0.54 mM ethylenediaminetetraacetic acid (EDTA), 0.5 g/L trypsin from bovine pancreas type-II-S; all Sigma-Aldrich). Proliferation medium consisted of Advanced DMEM/F12 (Invitrogen, Karlsruhe, Germany), 2 mM L-glutamine (Sigma-Aldrich), 1× N-2 supplement (Invitrogen), and 40 ng/mL recombinant basic fibroblast growth factor (bFGF, R&D Systems, Minneapolis, MN, USA). For differentiation, 6×10^6 LUHMES were seeded into a T175 flask in proliferation medium and differentiation was started after 24 hours (d0). Standard differentiation medium for G+ cells consisted of Advanced DMEM/F12, 2 mM L-glutamine, 1× N-2 supplement, 1 mM dibutyryl 3',5'-cyclic adenosine monophosphate (cAMP, Sigma-Aldrich), 1 μg/mL tetracycline (Sigma-Aldrich), and 2 ng/mL recombinant human GDNF (R&D Systems), whereas differentiation toward G− cells was achieved with medium lacking GDNF. After 48 hours of predifferentiation, LUHMES were trypsinized and transferred into multiwell plates at 1.4×10^5 cells/cm^2. Differentiation was continued for up to 8 days (d2–d10). For substitution experiments, 50-200 ng/mL human recombinant insulin-like growth factor 1 (IGF1; BioVision, Mountain View, CA, USA), 10-40 ng/mL recombinant human BDNF (R&D Systems), 20-60 ng/mL recombinant human beta NGF (R&D Systems), or 10-40 ng/mL recombinant human NRTN (R&D Systems) were added to the differentiation medium instead of GDNF. In titration experiments, 0.5-8 ng/ml GDNF or 5-80 ng/ml NRTN/NGF were applied to d8 LUHMES for 24 hours. Viability of cells under different conditions was regularly controlled by biochemical methods (resazurin reduction, lactate dehydrogenase release) and life cell staining as de-

scribed previously (Schildknecht et al., 2011; Stiegler et al., 2011).

2.3. RET knockdown

For knockdown experiments, we purchased two different *RET* small interfering (si)RNAs from Thermo Scientific Dharmacon (Lafayette, CO, USA): RET1: 5′-UGG CGA AGG CGA CGU CCG GUdT dT-3′; (Futami and Sakai, 2009); RET2: 5′-GGA GAA GAU GGU UAA GdTdT-3′, (designed using AiO bioinformatics software; Karreman, 2002). Furthermore, we used an siRNA against green fluorescent protein (*GFP*) as negative control (5′-GCA AGC UGA CCU GAA GUU TT-3′, Eurofins MWG Operon, Ebersburg, Germany). LUHMES were transfected on d2 in 12-well dishes with 100 nM siRNA, using Lipofectamine-2000 (LF; Invitrogen) according to the manufacturer's instructions. Briefly, for each 12-well, 2 μL LF and the siRNA were diluted separately in 75 μL Opti-MEM (Invitrogen) and incubated for 5 minutes at room temperature. Subsequently, the siRNA and LF mixtures were combined and complexes allowed to form for 20 minutes. During that time, d2 LUHMES were trypsinized and seeded into 12-well plates at 550,000 cells per well. Immediately after the plating step, 150 μL of the siRNA-lipid complexes were added per well. For a prolonged knockdown until d9, cell transfection was repeated on d6 by adding the siRNA-lipid complexes to the adherent cells after a medium change.

2.4. Immunocytochemistry

LUHMES on 15-mm glass cover slips were fixed on d0, d5, and d10 of differentiation with 4% paraformaldehyde in phosphate buffered saline (PBS) for 15 minutes at room temperature. After a 10-minute permeabilization step with 0.2% Triton X-100/PBS, cells were preincubated with 1% bovine serum albumin (BSA)/PBS (Calbiochem, San Diego, CA, USA) for 1 hour at room temperature. Subsequently, primary antibodies were added in 1% bovine serum albumin/PBS for overnight incubation at 4 °C (see Supplementary Fig. 1). Cells were then rinsed 3 times with PBS, and anti-rabbit Alexa-488 and anti-goat Alexa-488 (1:1000; Molecular Probes, Eugene, OR, USA) were applied as secondary antibodies for 1 hour at room temperature. After 3 washing steps, Hoechst-33342 (H-33342) (1 μg/mL; Molecular Probes) was added for 10 minutes and cover slips were then mounted on glass slides with Fluorsave reagent (Calbiochem). Samples were imaged with an Olympus IX 81 inverted epifluorescence microscope (Hamburg, Germany), using a 100× oil objective. Image processing was carried out with the Olympus Cell^{P} 3.3 software. For quantification of the neurite network density, cells were stained with 1 μM calcein-AM and 1 μg/mL H-33342 for 30 minutes at 37 °C. Image acquisition was carried out on an automated microplate reading microscope (Array-ScanII HCS Reader; Cellomics, Pittsburgh, PA, USA), and the total neurite area was normalized to the number of viable cells as already described (Stiegler et al., 2011).

2.5. Scanning electron microscopy

Scanning electron microscopy (SEM) was performed by Dr. J. Hentschel at the Electron Microscopy Service (EMS), University of Konstanz, as described previously (Scholz et al., 2011). Briefly, d5 and d10 LUHMES on 10-mm glass cover slips were fixed for 30 minutes with cold 2% glutaraldehyde/3% formaldehyde in 0.1 M pH 7.4 cacodylate buffer (0.09 M sucrose, 0.01 M $CaCl_2$ and 0.01 M $MgCl_2$; all Sigma-Aldrich). Samples were prepared for SEM, which was performed with a Philips SEM 505 (Eindhoven, The Netherlands) at 30 kV accelerating voltage. The digitally recorded images were processed with ImageJ 1.43s (National Institutes of Health, Bethesda, MD, USA; rsb.info.nih.gov/ij/) software.

2.6. Quantitative reverse-transcription polymerase chain reaction (PCR)

For quantitative reverse-transcription PCR (qPCR) analysis, total RNA was extracted by using the RNeasy mini kit (Qiagen, Hilden, Germany) according to manufacturer's instructions. Synthesis of cDNA from 1 μg of total RNA was carried out with Superscript II Reverse Transcriptase (Invitrogen) using random hexamers and oligodT primer. The cDNA was amplified using Platinum SYBR Green qPCR SuperMix (Invitrogen) and gene-specific primer pairs (Eurofins MWG Operon), listed in Supplementary Fig. 1. Alternatively, cDNAs were synthesized from 1 μg of total RNA, isolated from cells of 3 independent differentiations, by the RT^2 first strand kit (SABiosciences, Frederick, MD, USA). The cDNAs were separately analyzed with Human Alzheimer's Disease PCR Arrays (Cat. no. PAHS-057; SABiosciences), containing 84 preselected primer pairs for AD-related genes (see Supplementary Fig. 2). All qPCRs were run in a Bio-Rad Light Cycler (Bio-Rad, Munich, Germany) and analyzed with Bio-Rad iCycler software (iQ5 2.0). The expression level of each gene was calculated from the threshold cycle (ct) as relative expression compared with glyceraldehyde 3-phosphate dehydrogenase (*GAPDH*) ($2^{-\Delta ct}$) or as fold change relative to d0 ($2^{-\Delta\Delta ct}$) as already described (Scholz et al., 2011).

2.7. Western blotting

Samples were prepared as described earlier (Falsig et al., 2004). Briefly, cells were lysed in radioimmunoprecipitation assay (RIPA) buffer (50 mM Tris-base pH 7.5, 1 mM ethylenediaminetetraacetic acid (EDTA), 150 mM NaCl, 0.25% sodium deoxycholate, 1% Triton X-100, 1 mM Na_3VO_4, 50 mM NaF, 0.1% sodium dodecyl sulfate (SDS); all Sigma-Aldrich), supplemented with protease (Roche Diagnostics, Mannheim, Germany) and phosphatase (Sigma-Aldrich) inhibitors, for 15 minutes at 4 °C. After sonification and centrifugation of the samples, the protein

concentrations were determined with the Pierce BCA protein assay kit (Thermo Scientific, Rockford, IL, USA). Protein samples (20–30 μg) were boiled for 10 minutes with Laemmli buffer (pH 6.8, 63 mM Tris-HCl, 10% glycerol, 2% SDS, 0.0025% bromophenol blue; all Sigma-Aldrich) and separated by 10% Tris-glycine SDS polyacrylamide gel electrophoresis (PAGE). After transfer of the protein bands onto nitrocellulose membranes using the iBlot dry blotting system (Invitrogen), membranes were blocked with 3% milk in Tris-buffered saline/0.1% Tween (TBST) buffer for 1 hours at room temperature. Primary antibodies were then added in 3% milk in Tris-buffered saline/0.1% Tween overnight at 4 °C (see Supplementary Fig. 1). Membranes were rinsed and incubated for 1 hour at room temperature with goat anti-mouse and goat anti-rabbit (1:8000; Jackson Immuno Research Europe, Suffolk, UK), or rabbit anti-goat (1:10,000; Sigma-Aldrich) secondary antibodies, conjugated to horseradish peroxidase. After repeated washing, blots were visualized in a FUSION-SL 4.2 MP chemiluminescence system (Peqlab, Erlangen, Germany) using Pierce ECL Western blotting substrate (Thermo Scientific).

2.8. $A\beta_{1-40}$ and sAPPα/β quantification

Secreted $A\beta_{1-40}$ and sAPPα/β were always measured 24 hours after medium change in the conditioned supernatant of LUHMES cells. Aβ was directly detected by an $A\beta_{1-40}$-specific sandwich enzyme-linked immunosorbent assay (ELISA) kit (Invitrogen) (Volbracht et al., 2009). For sAPP quantification, 4 mL of supernatant were concentrated 20-fold with Amicon centrifugal filter units (Millipore, Billerica, MA, USA) before being applied to sAPPα- or sAPPβ-specific ELISAs (IBL International, Hamburg, Germany). Aβ and sAPP concentrations in the supernatants were normalized to the protein concentrations in the respective cell lysates. Typical product amounts per μg cell protein, released by G+ cells from d9 to d10, were 14.3 pg sAPPα, 7.8 pg sAPPβ, and 2 pg $A\beta_{1-40}$. For Western blotting of sAPPα/β, normalized volumes (25–30 μL, depending on the cellular protein content) of the concentrated supernatants were subjected to 8% Tris-glycine SDS polyacrylamide gel electrophoresis (PAGE) as described above.

2.9. Statistics

Experiments were repeated 2–6 times with different lots of cells. All data are displayed as means ± standard error of the mean unless indicated otherwise. Statistical analyses were performed by 1-way analysis of variance (ANOVA) with Dunnett's or Newman-Keuls post tests as appropriate, using the GraphPad Prism 4.0 software (San Diego, CA, USA). Data points were considered significantly different if $p < 0.05$. The half maximal inhibitory concentration (IC_{50}) values were derived from curves obtained by sigmoidal dose-response curve fitting (GraphPad Prism).

3. Results

3.1. Expression and maturation of AD-relevant markers during differentiation

For characterization of AD-related marker expression in LUHMES cells, we quantified the levels of 86 AD-relevant messenger (m)RNAs in proliferating (d0), differentiated (d5), and in aging (d10) cells (see Supplementary Fig. 2 for complete data). Already at the neuronal precursor cell stage (d0), APP family genes and components of the α-, β- and γ-secretases were expressed at high levels (relative to *GAPDH* and other neural genes). Only *BACE2* levels were below the detection limit. During differentiation, *BACE1*, *PSEN1*, and *APP* were upregulated approximately 4-fold on d5, and then remained at that level until d10 (Fig. 1A). Some nonprotease genes involved in APP turnover, such as *APOE* or *LRP1*, were more weakly expressed on d0, but also more dynamically regulated during differentiation than the other genes (Fig. 1A).

When protein levels of BACE and APP were examined on d0 and d2, we found that they were mostly present in their immature, low molecular weight forms with only partial posttranslational modifications (Fig. 1B). The majority of the detected BACE proteins still carried the propeptide, which is known to be cleaved off during or after the passage through the Golgi apparatus. From d4 onward, increased protein amounts (APP and BACE) and a shift from the immature to the mature forms were detectable. No further changes occurred until d10 (Fig. 1B). The latter finding correlated well with the mRNA data, showing a steady state situation from d5 onward. In summary, LUHMES express increasing amounts and progressively maturing forms of AD-relevant proteins during differentiation, and cells at different stages may be used to study human APP and BACE in their different posttranslationally modified forms without need for ectopic expressions.

3.2. Modulation of proteolytic processing of APP in differentiated LUHMES

As the pathophysiology of APP is closely linked to its proteolytic processing, we examined the latter process during the differentiation of LUHMES. At an early stage of differentiation, α- and β-secretase activity appeared to be low, as soluble APPα (sAPPα) and soluble APPβ (sAPPβ) were found in only very low amounts in the culture supernatants (Fig. 2A). The concentration of secreted $A\beta_{1-40}$ was also low (Fig. 2B). Until d5, generation of all protein fragments strongly increased, and the secretion of Aβ and sAPPβ further augmented until d10 (Fig. 2A and B) in spite of constant expression of the main genes/proteins (Fig. 1). Thus, d5 LUHMES express a fully developed machinery for the processing of endogenous APP and the generation of amyloidogenic peptides.

To further qualify LUHMES cells as a model to study AD-relevant processes, we tested some pharmacological

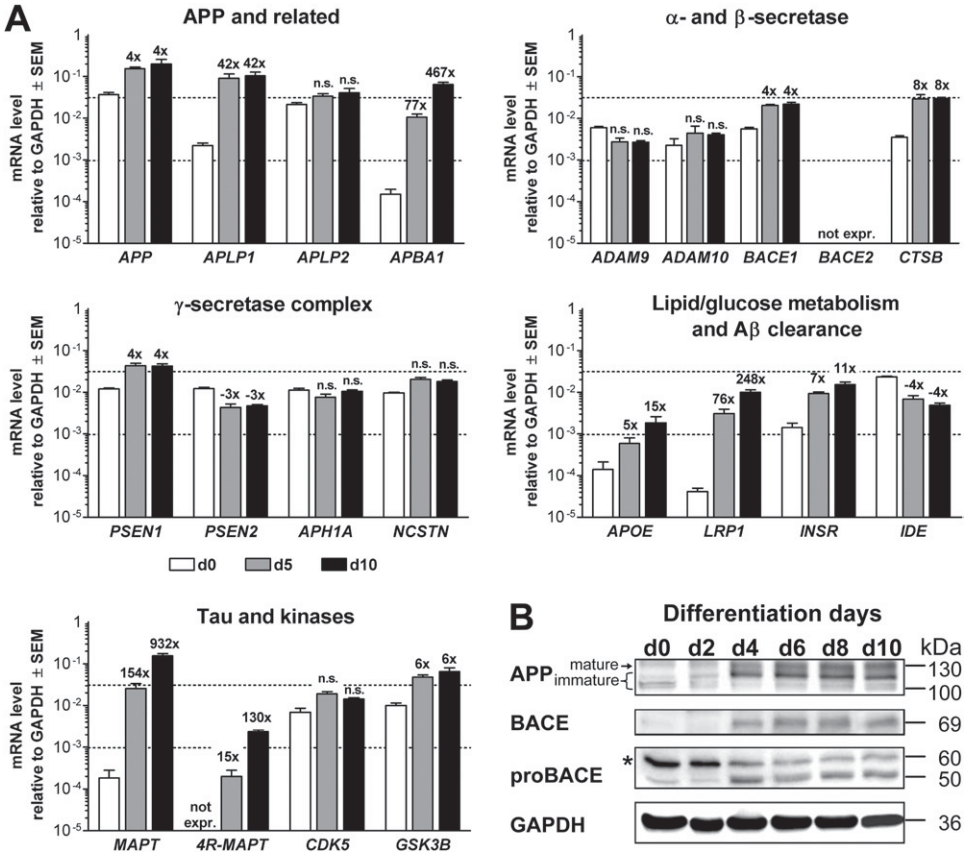

Fig. 1. Changes of Alzheimer's disease (AD)-related messenger (m)RNAs and proteins during differentiation. (A) Transcript levels in day (d)0, d5 and d10 LUHMES were analyzed by quantitative reverse-transcription polymerase chain reaction (qPCR). Data are displayed relative to glyceraldehyde 3-phosphate dehydrogenase (*GAPDH*) mRNA levels and are means ± standard error of the mean of 3 independent differentiations. The regulation factors on d5/d10 relative to d0 (x-fold regulation) are indicated above the bars. Where numbers are indicated, the regulation was significant ($p < 0.05$). Nonsignificant changes are marked by "n.s." The abbreviations are the official gene symbols according to the HUGO gene nomenclature committee (HGNC) database; *4R-MAPT* refers to the long *MAPT* isoform with exon 10 included. (B) Lysates were obtained from differentiating cells at different stages and analyzed with 3 different antibodies (with GAPDH as loading control) by Western blot analysis. The amyloid precursor protein (APP) antibody recognized 3 bands corresponding to immature and mature forms of the protein. The β-secretase (BACE) antibody stained primarily the mature glycosylated protein, whereas the serum raised against the BACE propeptide (proBACE) only recognized immature BACE forms with no, or with partial (asterisk) glycosylation.

interventions known to affect Aβ generation in other systems. First, we depleted the cells of cholesterol, because this has been reported to lead to reduced Aβ generation due to disorganization of lipid rafts and a subsequent redistribution of APP and BACE (Guardia-Laguarta et al., 2009; Simons et al., 1998). Indeed, we found that treatment of cells for 1–2 days with the cholesterol synthesis inhibitor simvastatin in combination with the cholesterol chelator methyl-β-cyclodextrin resulted in a significant decrease in secreted Aβ (Fig. 2C). The applied concentrations of the drugs were noncytotoxic, and the effect was rescued by the readdition of cholesterol (not shown). In a second set of experiments, we incubated LUHMES with cell permeable BACE and γ-secretase inhibitors. Inhibition of BACE with IPAD resulted in a block of Aβ generation with an IC_{50} of 2 nM, as expected from other neuronal systems (Volbracht et al., 2009) (Fig. 2D). Inhibitors of γ-secretase also reduced Aβ levels in the nanomolar range and the pharmacological efficacy of all drugs was similar in d5 and d10 cells (Supplementary Fig. 3). To further probe the site of APP processing by BACE, we used the highly potent (K_i value = 1.6 nM), but cell impermeable, BACE inhibitor OM99-2 (Gosh et al., 2000). This compound did not lower Aβ levels unless micromolar concentrations were used (IC_{50} = 2 μM) (Fig. 2D). These findings suggest that APP and/or BACE reside in cholesterol-rich membrane compartments ("lipid rafts") in LUHMES and that APP cleavage mainly takes place in an intracellular compartment. In this respect, the LUHMES cell model is similar to primary neurons.

3.3. Increased Aβ production in aged LUHMES is independent of tau changes

As we were interested in the cellular changes causing the increase of Aβ secretion in aging cells, we asked whether increased Aβ was linked to the morphology of neurites and to the expression or phosphorylation status of microtubule associated protein tau (MAPT). Our qPCR analyses re-

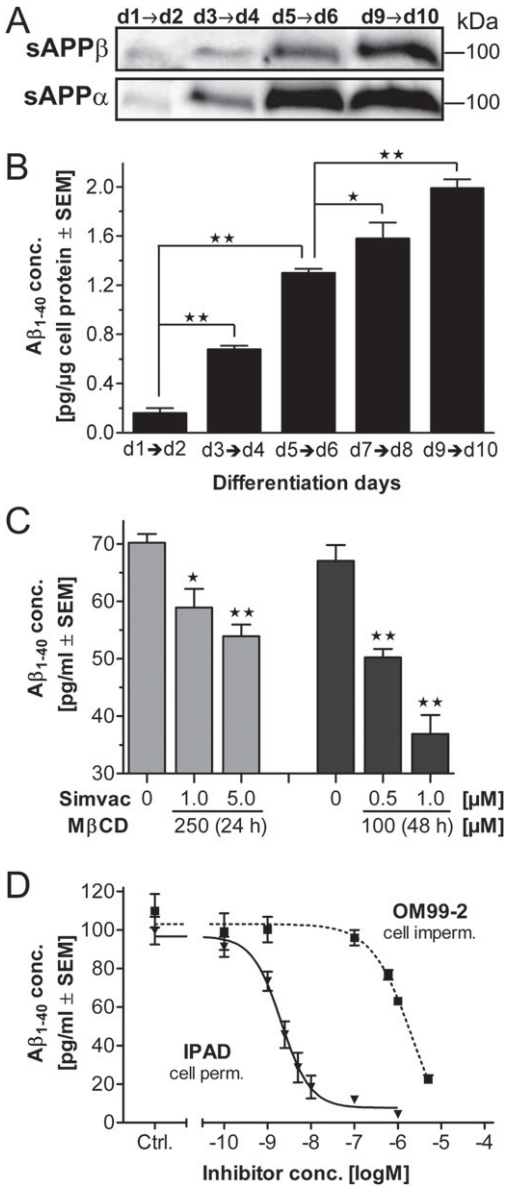

Fig. 2. Proteolytic amyloid precursor protein (APP) processing during differentiation and cell treatment. (A) Conditioned medium was collected from LUHMES cultures at different time points of differentiation. Differentiation day (d)1→d2, for instance, indicates that medium was changed on d1 and the supernatant was sampled 24 hours later on d2. The amounts of soluble (s)APPα and sAPPβ in a defined medium volume were analyzed by Western blot. One experiment representative for 3 is shown. (B) Amyloid β $(A\beta)_{1-40}$ was measured by enzyme-linked immunosorbent assay (ELISA) in supernatants as described in (A). The data were normalized to the protein concentrations of the respective cell lysates in the well from which the supernatant was sampled and are indicated in pg Aβ per μg cellular protein. (C) LUHMES (d5) were treated for 24 hours with 250 μM methyl-β-cyclodextrin (MβCD) or for 48 hours with 100 μM MβCD together with various nontoxic concentrations of simvastatin (Simvac) as indicated. Then, medium was changed, and simvastatin (but not MβCD) incubation was continued, and the supernatants were analyzed 24 hours later for secreted $A\beta_{1-40}$. (D) LUHMES (d9) were treated after a medium change with the cell permeable small molecule β-secretase (BACE) inhibitor isophtalamide derivative (IPAD) or with the cell-impermeable peptidic inhibitor OM99-2. After 24 hours, $A\beta_{1-40}$ was analyzed in the conditioned supernatant by ELISA. Data in (B–D) are mean ± standard error of the mean (n = 3–6). * $p < 0.05$, ** $p < 0.01$.

vealed that *MAPT* expression from d0–d10 displayed the strongest regulation pattern of all genes investigated (Fig. 1A). As different isoforms of tau are known to be developmentally regulated (Buée et al., 2000), we also used a primer pair only annealing to the 4-repeat-(4R-) tau transcripts involved in tau pathology. Expression of these transcripts was below the detection limit on d0, and then strongly increased during the next days. Thus, only 3-repeat forms, including fetal tau, were expressed in d0 LUHMES, and the expression pattern changed with time (Fig. 1A). This may be linked to prominent changes in the neurite network, which became denser but also more fragile between d5 and d10, as revealed by βIII-tubulin immunostaining and scanning electron microscopy (Fig. 3A). To obtain more information, tau protein expression and phosphorylation were analyzed by Western blot with epitope-specific antibodies. The tau-1 antibody recognized bands of several tau isoforms, not phosphorylated on serine 202/threonine 205 (AT8 epitope), and the levels of most of these isoforms increased from d0 to d10 (Supplementary Fig. 4). In parallel, a high-molecular weight form, strongly phosphorylated at the AT8 epitope, and 1–3 bands of lower molecular weight with phosphorylation on serine 396 (Ser396) were present in d10 samples, but much less on d5 (Fig. 3B). These changes, occurring from d5 to d10, could be mimicked by short treatment of d5 cells with okadaic acid (Supplementary Fig. 4). This toxin inhibits protein phosphatase 2A (PP2A), an enzyme which dephosphorylates tau and that may be linked to the pathology of AD. In order to test whether the increased Aβ generation was causing tau phosphorylation, or vice versa, we used the γ-secretase inhibitor LY450139 and the compound CHIR98014 that selectively blocks glycogen synthase kinase 3 (GSK3), one of the tau-phosphorylating kinases. The kinase inhibitor blocked phosphorylation of Ser396 and attenuated the one of AT8, while the secretase inhibitor did not affect tau phosphorylation (Fig. 3C). When the Aβ release was quantified, CHIR98014 had no effect on the increased production on d10, while LY450139 blocked it (Fig. 3D). Moreover, treatment with okadaic acid did not increase Aβ secretion from d5 cells (Supplementary Fig. 4). Together, these data strongly suggest that the observed changes in tau phosphorylation, possibly related to neurite changes in aging LUHMES, are not the cause of the increased Aβ production in d10 cells—and that Aβ production is not causally involved in the augmented tau phosphorylation.

3.4. Enhanced APP processing and RET expression in the presence of GDNF

We explored the hypothesis that factors in the differentiation medium might be responsible for the continuous increase of Aβ production after d5, when mRNA/protein levels themselves were mostly constant. In order to test the role of GDNF, we grew the cells in the absence of this factor (G− medium), and compared them with cells in the normal differentiation

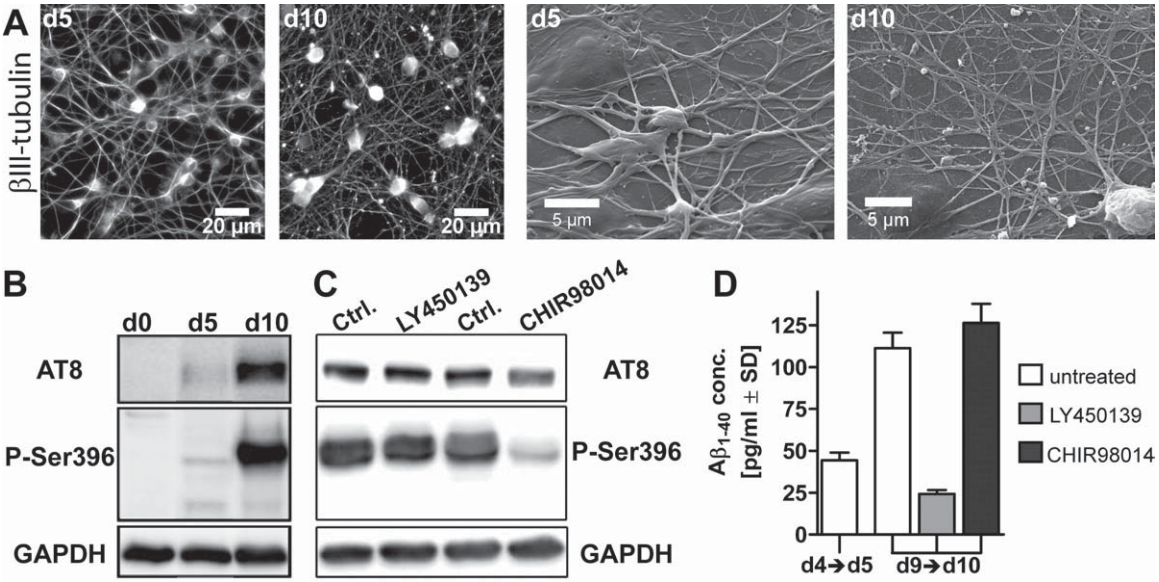

Fig. 3. Pharmacological uncoupling of tau phosphorylation and amyloid β (Aβ) generation. (A) Representative βIII-tubulin immunostainings (left) and scanning electron microscopy (SEM) images (right) of day (d)5 and d10 LUHMES. Note the finer, more delicate and branched network as well as the more pronounced rounding of cell bodies on d10. (B) Cell lysates were prepared on different days of differentiation and analyzed for changes of tau by Western blot. Analysis with the AT8 antibody indicated phosphorylation of serine 202/threonine 205 on d10. The P-Ser396 antibody detected a 50 kDa form of tau, phosphorylated at serine 396. (C) LUHMES were incubated on d9 either with solvent (Ctrl.) or with the γ-secretase inhibitor LY450139 (1 μM) or the glycogen synthase kinase 3 (GSK3) inhibitor CHIR98014 (2 μM). After 24 hours, protein lysates were prepared and analyzed by Western Blot for AT8, P-Ser396, and GAPDH (loading control). (D) The experiment was performed as in (C), and the $A\beta_{1-40}$ concentration was measured in the supernatants of the cells (d9→d10). For comparison, the $A\beta_{1-40}$ concentrations were also quantified for d5 cells (d4→d5) in the same experiments. Data are mean ± standard error of the mean (n = 2) and images/blots are representative for 2 independent experiments.

medium (G+ medium, containing 2 ng/mL GDNF) (Fig. 4A). The cells, grown in G− medium (G− cells), released similar amounts of Aβ as G+ cells until d5. However, the increase, normally seen in G+ cells at later time points (d7–d10), was abolished in G− cells (Fig. 4B). For further analysis, we quantified α- and β-secretase cleavage products of APP with highly specific ELISAs. The data indicate a significant decrease in sAPPβ levels in G− cells, while sAPPα generation of G− cells was slightly but not significantly stronger than in G+ cells (Fig. 4C). These findings may be explained by increased β-/γ-secretase activities. Alternatively, the release of cleavage products from cells may be affected. Therefore, we also measured $A\beta_{1-40}$ and sAPPβ in cell lysates. Their levels were not quantifiable as they were at or below the detection limit, both in G+ and G− cells.

To investigate whether an alteration of gene expression and overall cell differentiation was causing the effects, we compared the mRNA levels of 88 neuronal and AD-relevant genes in d10 G+ and G− cells and found none of 87 genes varying significantly between G− and G+ conditions. This also included *APP, BACE*, all other secretase components, *MAPT*, several kinases, the GDNF binding receptor *GFRA1*, tyrosine hydroxylase (TH), and the neuronal marker *FOX-3*. The only exception was the receptor tyrosine kinase *RET* (Fig. 5A). We also examined the protein levels of APP and BACE, and no evident differences in protein expression or localization of APP and BACE were observable by immunocytochemistry or Western blot analysis (Fig. 5B and C). To examine *RET* expression in more detail, we analyzed mRNA levels in G− and G+ cells over the entire time course of differentiation. The main upregulation phase of *RET* started on d5, with a 3.5-fold difference between G− and G+ detectable from d8 onward (Fig. 5D). On protein level, this was visualized as a strongly RET-immunoreactive subpopulation of G+ LUHMES, which was lacking in G− cultures (Fig. 5E). In summary, the presence of GDNF resulted in increased levels of the APP-derived cleavage products Aβ and sAPPβ, and in enhanced RET expression in d5–d10 LUHMES, while mRNA transcription of a very broad range of other genes remained unaffected.

3.5. Triggering of increased Aβ in mature LUHMES by RET-activating ligands

Having identified GDNF as a factor increasing Aβ release, we investigated whether other neurotrophins would show similar activity. First, we checked in G− cells the mRNA levels of several growth factor receptors by qPCR and found that all of them were expressed at the latest on d5 and then either further upregulated (*TrkA/B, GFRA2*) or stably expressed (*IGF1R, GFRA1*) (Fig. 6A). We also found that neither G+ nor G− LUHMES expressed any endogenous *GDNF* mRNA at any time point, whereas for example endogenous *BDNF* mRNA was detected in increasing amounts from d0–d10 (Supplementary Fig. 2).

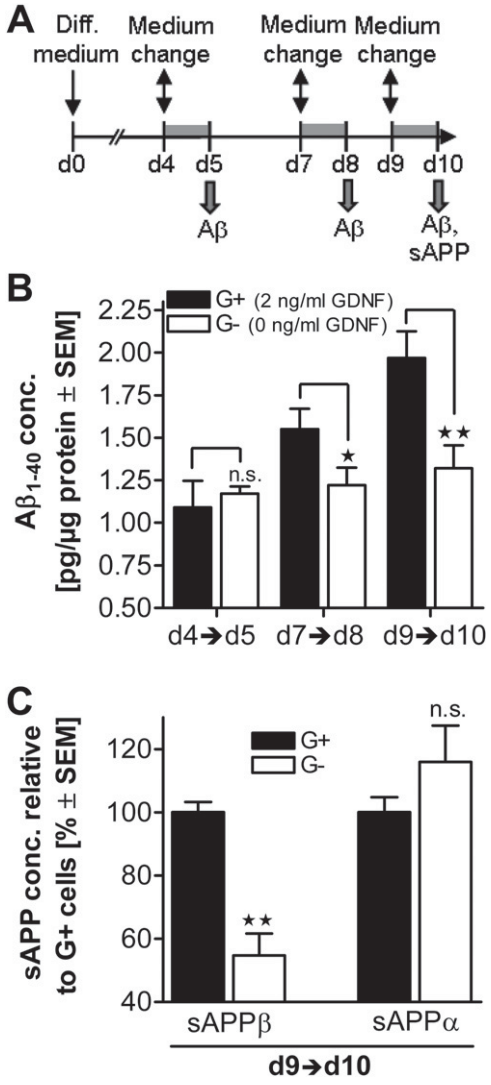

Fig. 4. Modulation of amyloid precursor protein (APP) processing by glial cell line-derived neurotrophic factor (GDNF). (A) Schematic representation of the experimental procedure used below. LUHMES were differentiated for 10 days in normal medium containing 2 ng/mL GDNF (G+) or in medium without GDNF (G−). At the time points indicated, the cells received fresh medium, and 24 hours later (gray bars), the conditioned supernatants were analyzed for accumulated peptides (e.g., d4→d5). (B) Supernatants from cells, grown in G+ or G− medium, were analyzed for amyloid beta $(A\beta)_{1-40}$ as described in Fig. 2. (C) Supernatants were analyzed for either soluble (s)APPα or sAPPβ by enzyme-linked immunosorbent assay (ELISA). The data were normalized to the protein concentrations of the respective cell lysates and are displayed relative to the values obtained for G+ cells. All data are mean ± standard error of the mean (n = 6–8). * $p < 0.05$, ** $p < 0.01$.

We were interested whether the late increase of Aβ was also triggered by GDNF or other factors when these were added only to mature cells (from d5 onward). We supplemented d5 G− cells with either GDNF, its close relative NRTN, or NGF, all of which are able to directly or indirectly activate RET. Alternatively, we used growth factors signaling exclusively through their own receptors, namely BDNF and IGF1 (Fig. 6B and C). Determination of the $A\beta_{1-40}$ concentration in the supernatant of d10 cells showed that it was significantly increased in comparison with G− cells when GDNF, NGF and NRTN were added. The addition of GDNF on d5 was as efficient as the continuous presence of GDNF from d0–d10 (Fig. 6C). In contrast, incubation of G− cells with medium containing IGF1 or BDNF did not result in any significant increase in Aβ generation (Fig. 6C). Notably, when we depleted G+ cells of GDNF from d5 to d10 to test the reversibility of the effect, we found that Aβ production considerably decreased to similar levels as in G− cells (Fig. 6C). These data demonstrate that GDNF and related RET-signaling factors are necessary and sufficient to trigger a late increase in Aβ levels and that this effect can be switched on or off in mature d5–d10 LUHMES.

3.6. Reduced Aβ generation in response to RET knockdown or inhibition

In order to corroborate the proposed role of RET in Aβ generation, we performed knockdown (KD) experiments both in young (d2–d5) and old (d6–d9) G+ LUHMES, using 2 different *RET* siRNAs. Quantification of *RET* mRNA levels revealed that *RET* expression was reduced by about 50% in both conditions, while *GFP* siRNA worked as nonspecific control (Fig. 7A). The mRNA data were confirmed on protein level by Western blot analysis. Notably, the RET levels of KD G+ cells were reduced to a similar extent as those of G− cells (Fig. 7B). In d5 cells, RET KD did not affect the amount of secreted $A\beta_{1-40}$. In contrast to this, we observed a significant reduction of $A\beta_{1-40}$ in the supernatants of KD d9 cells. These data indicate that RET signaling is only important for Aβ release from older cells. We used a pharmacological approach to further confirm the results obtained by RET KD. G+ cells were incubated from d6 to d9 with the RET inhibitor RPI-1 (Cuccuru et al., 2004). The amount of Aβ in the supernatant was reduced with increasing inhibitor concentrations, with a maximum decrease of approximately 50% (Fig. 7D). Western blot analysis of the RET downstream target protein kinase B (AKT) revealed reduced amounts of phosphorylated AKT in RPI-1 treated cells compared with control cells, showing that RET signaling was efficiently inhibited by the compound (Fig. 7E). In summary, these data confirm our hypothesis that the observed Aβ increase in response to GDNF stimulation is mediated by RET in older (d9), but not in young (d5) LUHMES cells.

3.7. Immediate trigger of Aβ secretion by RET-signaling factors

We investigated whether neurotrophic factors would trigger enhanced Aβ production without preincubation for several days, and whether this was dose-dependent. For this purpose, cells were kept in G− medium for 8 days, and the factors were then added for only 24 hours. In a parallel set

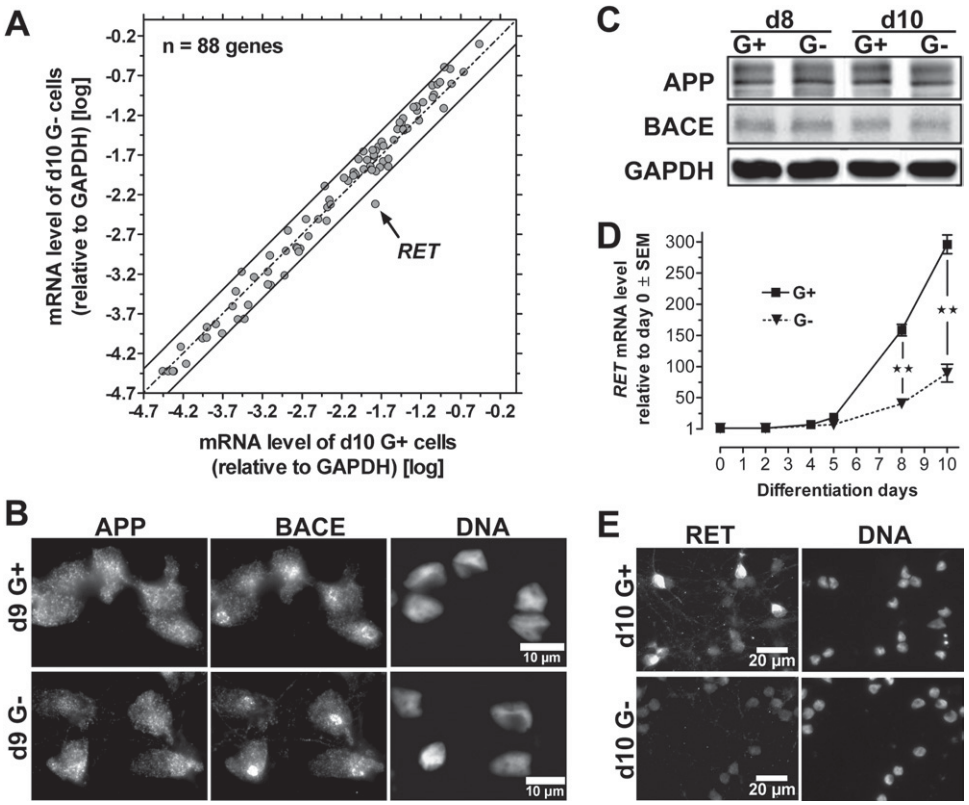

Fig. 5. Selective effects of glial cell line-derived neurotrophic factor (GDNF) on "rearranged during transfection" (RET) expression. (A) RNA was isolated from LUHMES that had been grown for 10 days in medium without GDNF (G−) or with GDNF (G+). The transcript levels (relative to *GAPDH*) were quantified for 88 genes by quantitative reverse-transcription polymerase chain reaction (qPCR). Data are presented in a scatter plot with logarithmic axes. The dashed line indicates equal expression under both conditions. The 2 solid lines indicate 2-fold differences in gene expression between G+ and G− samples. The only gene that was significantly differentially expressed was *RET* (arrow). (B) Immunostaining of day (d)9 G+ and G− cells for amyloid precursor protein (APP) and β-secretase (BACE). DNA was labeled with Hoechst dye H-33342. (C) Western blot detection of APP and BACE in cell lysates of LUHMES, grown for 8–10 days in G+ or G− medium. (D) The mRNA expression levels of *RET* were determined by qPCR at the indicated days of differentiation for G+ and G− cells and are displayed relative to d0 on a linear scale. (E) Cells, grown in G+ or G− medium, were immunostained on d10 for RET. DNA was labeled with H-33342. Data in (A) and (D) are mean ± standard error of the mean of 3 independent differentiations. ** $p < 0.01$. Blots/images in (B), (C) and (E) are representative for 3 experiments.

of experiments, d8 G+ cells were used to test whether a further increase in neurotrophic factors would also further boost Aβ secretion (Fig. 8A). Addition of increasing concentrations of GDNF to G− cells resulted in an increase of Aβ at optimum concentrations of about 2 ng/mL (= 134 pM monomer), and to a loss of the effect at higher concentrations (Fig. 8B). Also for NGF and NRTN, there was a defined concentration window in which supplementation resulted in the described Aβ increase in G− cells, with optimum concentrations of 40 ng/mL NGF and 20 ng/mL NRTN (Supplementary Fig. 5). Notably, also G+ cells were stimulated by additional GDNF to produce 30% more Aβ (Fig. 8B, right). G+ cells, supplemented with a total of 3–4 ng/mL GDNF, produced about 200% Aβ compared with G− cells. Both in G− and in G+ cells, the increased Aβ production in response to GDNF was paralleled by a decreased release of sAPPα. High concentrations of GDNF, which did not lead to augmented Aβ production, did also not affect sAPPα (Fig. 8C). To a certain degree, the regulation of *RET* mRNA levels paralleled these effects. Supplementation of G− cells with optimal GDNF concentrations, triggering an Aβ increase, was accompanied by a strong upregulation of *RET*, while "overdoses" of GDNF did not significantly upregulate *RET* (Fig. 8C, left). In G+ cells, there was no significant increase in *RET* mRNA expression at any given concentration of GDNF (Fig. 8C, right), possibly because the maximal level had already been reached. In agreement with this assumption, the acute depletion of GDNF from G+ cells resulted in an immediate reduction of the *RET* mRNA level (Fig. 8C, right). Possible sAPPβ alterations were not quantifiable in the GDNF addition/deprivation experiments, most likely due to the short accumulation time and the lower overall levels.

For a direct comparison of the neurotrophic factors, we incubated d8 G− cells with the respective optimal concentrations of 3 neurotrophins for 24 hours. Significantly raised Aβ concentrations were detected in all supernatants, with a rank order of the stimuli of NGF < NRTN < GDNF. This

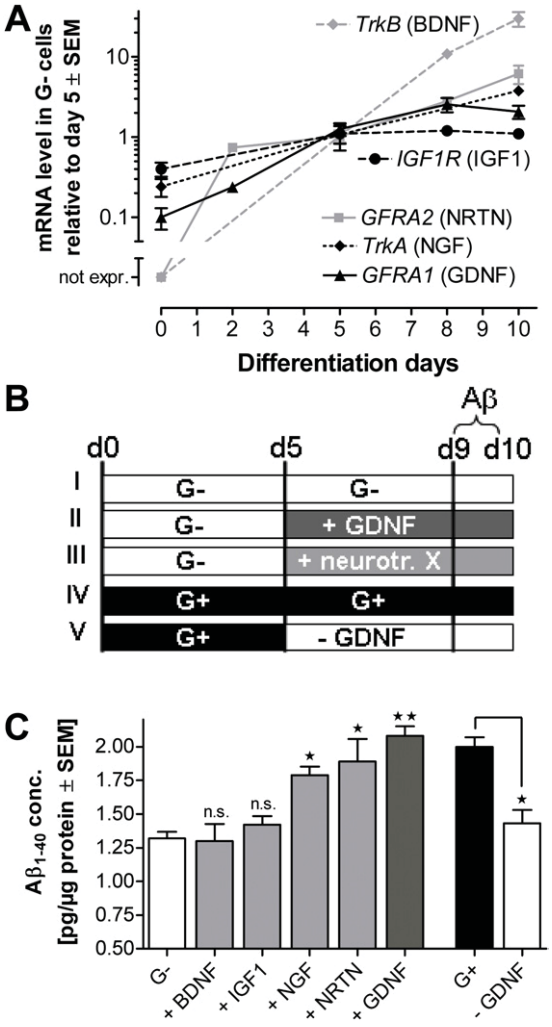

Fig. 6. Increased production of amyloid β (Aβ), triggered by glial cell line-derived neurotrophic factor (GDNF). (A) RNA was prepared from LUHMES cells grown in medium without GDNF (G−) on various days of differentiation. The expression levels of genes coding for growth factor receptors were quantified and the data are indicated relative to the levels on day (d)5. The neurotrophic peptides, expected to bind to the respective receptors, are indicated in brackets. (B) Schematic representation of the experimental approach below. (I–III) LUHMES were differentiated from d0 to d5 in G− medium (without GDNF). From d5 to d10, the G− condition was continued (I), or 2 ng/mL GDNF were added (II), or another neurotrophic factor (neurotr. X) was added (III): 20 ng/mL brain-derived neurotrophic factor (BDNF), 50 ng/mL insulin-like growth factor 1 (IGF1), 40 ng/ml NGF or 20 ng/ml NRTN. (IV–V) As reverse control, cells were incubated in G+ medium (2 ng/mL GDNF) from d0 to d5. Then, GDNF was added further (IV), or was withdrawn (V). Aβ generation was measured in all cases after the last 24 hours. (C) Measurement of Aβ secretion (normalized to cellular protein) in cells grown under the conditions described in (B). Data are mean ± standard error of the mean ($n = 3$). * $p < 0.05$, ** $p < 0.01$; "n.s." refers to no statistically significant difference compared with the G− control. Abbreviations: *GFRA1/2*, GDNF family receptor Alpha 1/2; *IGF1(R)*, insulin-like growth factor 1 (receptor); NGF, nerve growth factor; NRTN, neurturin; *TrkA/B*, neurotrophic tyrosine kinase receptor type 1/2 (*NTRK1/2*).

regulation of Aβ was paralleled by an increase in *RET* mRNA with similar rank order of the neurotrophic peptides (not significant in the case of NGF) (Fig. 8D). Upregulation

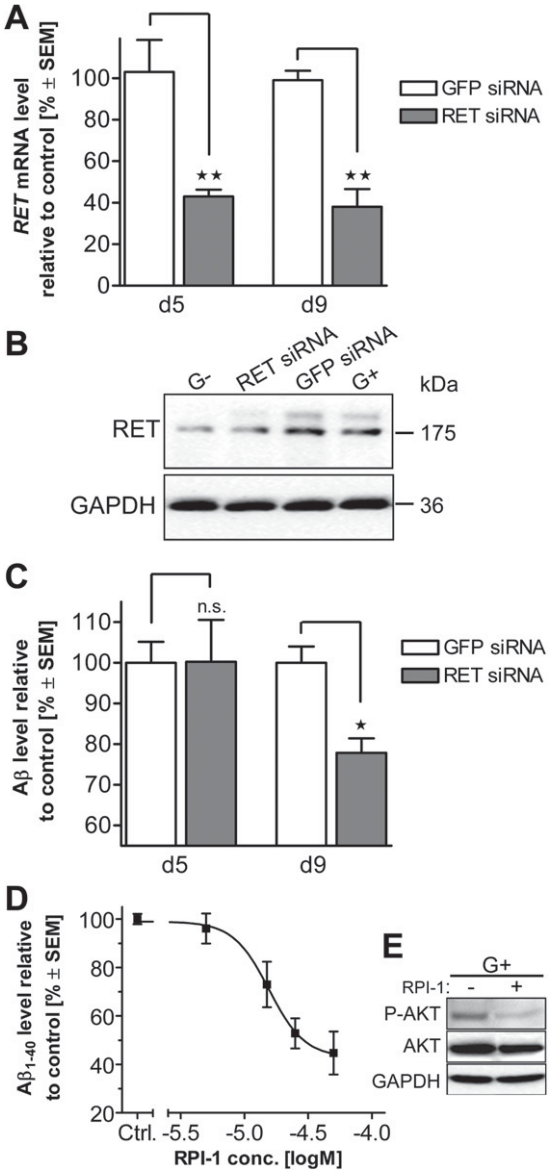

Fig. 7. Effects of "rearranged during transfection" (RET) knockdown or RET inhibition on amyloid β (Aβ) generation. (A) Cells grown in medium with glial cell line-derived neurotrophic factor (GDNF) (G+) were transfected on day (d)2, or on d2 and d6 with *RET* or green fluorescent protein (*GFP*) small interfering (si)RNA. Three days after the last transfection, RNA extracts were prepared and analyzed for *RET* mRNA expression by quantitative reverse-transcription polymerase chain reaction (qPCR). Average values of 2 different siRNAs are displayed relative to *GFP* siRNA controls. (B) Cell lysates were prepared from d9 cells grown in medium without GDNF (G−)/G+ control cells and from G+ cells, which had been transfected with *GFP* or *RET* siRNA. Samples were analyzed for RET expression by Western blot, GAPDH served as loading control. (C) Detection of $A\beta_{1-40}$ in supernatants of G+ cells treated as in (A), 24 hours after a medium exchange. Data are shown relative to *GFP* siRNA control. (D) G+ cells were treated from d6 to d9 with different concentrations of the RET inhibitor RPI-1. After a medium change on d8 (and fresh addition of RPI-1), the supernatants were analyzed 24 hours later for secreted $A\beta_{1-40}$. Data are displayed relative to untreated control cells. (E) G+ cells either were left untreated or were treated with 50 μM RPI-1 from d6 to d9, and cell lysates were analyzed on d9 for protein kinase B (AKT) and phospho-AKT (P-AKT). GAPDH served as loading control. All data are mean ± standard error of the mean ($n = 3$). * $p < 0.05$, ** $p < 0.01$.

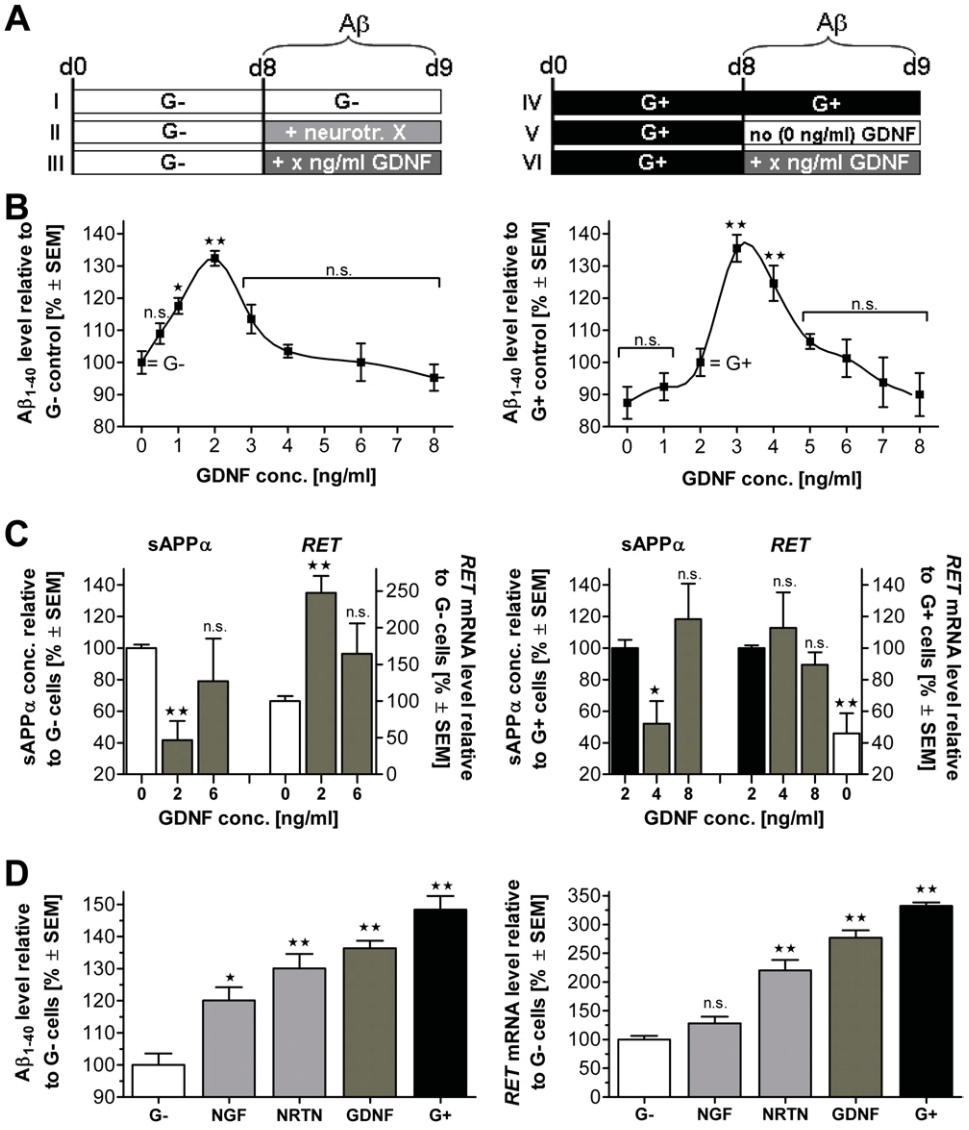

Fig. 8. Rapid regulation of amyloid β (Aβ) production by "rearranged during transfection" (RET) ligands. (A) Schematic representation of the experimental approaches below. Cells were grown from day (d)0 to d8 in medium without (G−) or with glial cell line-derived neurotrophic factor (GDNF) (G+). Neurotrophic factors (neurotr. X) or different concentrations of GDNF (no GDNF or x ng/mL GDNF) were added only for 24 hours from d8 to d9, and Aβ accumulation in the medium during this time was monitored. (B) G− (left) or G+ (right) cells were incubated from d8 to d9 with media containing various concentrations of GDNF as indicated (conditions III, V, and VI in A). Supernatants were analyzed after 24 hours for $A\beta_{1-40}$ and data are displayed relative to the Aβ generation of the respective G− or G+ controls (conditions I and IV). (C) G− (left) or G+ (right) cells were treated as in (B). After 24 hours, soluble amyloid precursor protein (sAPP)α was detected in the supernatants, and *RET* expression was quantified by quantitative reverse-transcription polymerase chain reaction (qPCR) after RNA isolation from cell lysates. (D) G− cells were incubated from d8 to d9 with the experimentally determined optimal concentrations of neurotrophic factors: 40 ng/mL nerve growth factor (NGF), 20 ng/mL neurturin (NRTN), 2 ng/mL GDNF (conditions II, III). Left: Aβ was measured and is displayed relative to G− controls. Right: On d9, *RET* mRNA levels were determined by qPCR and normalized to *GAPDH*. They are shown relative to the *RET* mRNA levels of G− controls. All data are mean ± standard error of the mean (n = 3–6). * $p < 0.05$, ** $p < 0.01$, "n.s." refers to no statistically significant difference to the respective G+ or G− controls.

of *RET* by GDNF also took place on the protein level as revealed by immunocytochemistry and Western blot (Supplementary Fig. 5).

Taken together, these experiments demonstrate that triggers of RET signaling can increase Aβ production and reduced sAPPα release within 24 hours. Moreover, downward changes of Aβ production after GDNF withdrawal are slower than the upward changes after addition of GDNF, while *RET* expression is quickly regulated by increased or decreased receptor stimulation.

3.8. Identification of the PI3K/AKT/mTOR pathway as contributor to GDNF-triggered Aβ increase

In order to obtain information on downstream effectors of the GDNF-RET signaling cascade, we examined whether specific inhibitor compounds would block the GDNF-stim-

ulated Aβ increase. When d8 G− cells were treated with the protein kinase C (PKC) inhibitor bisindolylmaleimide 1 (Bis1) during the period of GDNF addition, we found no significant difference in Aβ generation between control and Bis1-treated cells (Fig. 9A). This is consistent with our finding that the PKC activator phorbol 12,13-dibutyrate did not mimic GDNF effects (Supplementary Fig. 6). The GDNF-triggered Aβ increase was also not affected by incubation of the cells with the Src kinase inhibitor SU6656; it was slightly attenuated by the MEK1/2 inhibitor U0126 (Fig. 9A). A complete prevention of any Aβ elevation was observed after application of the RET inhibitor RPI-1, the phosphatidylinositol-3-kinase (PI3K) inhibitors wortmannin or PIK-90, or the mammalian target of rapamycin (mTOR) inhibitor rapamycin (Fig. 9A). Similar data were also obtained in a variation of the experiment, when G+ cells were treated with the inhibitors. Block of PI3K or mTOR in such cells, continuously exposed to GDNF, resulted in a strong decrease of Aβ—similar to or even stronger than after deprivation of GDNF. U0126 did not significantly lower Aβ generation in this setup (Supplementary Fig. 6). Incubation of G− cells with the same compounds in the absence of GDNF did not significantly affect Aβ generation (Supplementary Fig. 6). These data indicate that the inhibitors do not affect the basal Aβ generation, and that their effect is related only to the enhanced production in the presence of RET ligands. Based on these findings, we hypothesized that the primary RET downstream target, involved in the GDNF-mediated Aβ increase, was the PI3K/AKT/mTOR signaling cascade. In order to obtain biochemical evidence for the activation of this pathway, the levels of AKT and phosphorylated (P-) AKT were analyzed by Western blot. P-AKT was significantly decreased in G− compared with G+ cells (Fig. 9B and C). Moreover, GDNF supplementation resulted in a strong increase of AKT phosphorylation, which was blocked by the treatment of the cells with wortmannin or PIK-90. Rapamycin, which blocks mTOR downstream of P-AKT, did not reduce GDNF-triggered AKT phosphorylation (Fig. 9B and C). Altogether, these data strongly suggest that GDNF-triggered RET-signaling augments Aβ secretion in older (d5–d10) LUHMES cultures through the activation of the PI3K/AKT pathway, which leads further downstream to the activation of the rapamycin-sensitive mTOR complex 1.

4. Discussion

Based on the current study, we propose a dual regulation model for APP processing in human LUHMES neurons. The two main factors are (1) the differentiation status, which plays a predominant role in young cells, and (2) GDNF-stimulated RET signaling, which dominates at later stages of fully postmitotic cells. We found that differentiation of LUHMES cells during the initial 5 days was linked to an upregulation of AD-related genes and a maturation of

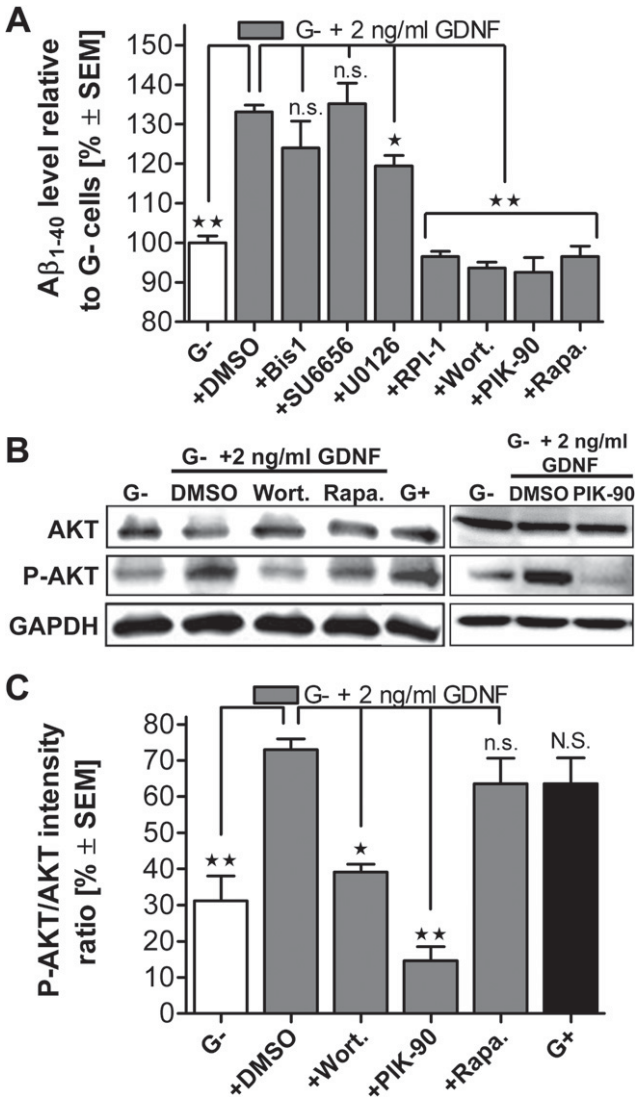

Fig. 9. "Rearranged during transfection" (RET)-triggered AKT phosphorylation and amyloid β (Aβ) generation. (A) LUHMES were grown in medium without glial cell line-derived neurotrophic factor (GDNF) (G−) for 8 days. Then, Aβ generation was measured from day (d)8→d9 in cells without GDNF or in cells supplemented with GDNF plus various pharmacological compounds: dimethyl sulfoxide (DMSO; solvent), protein kinase C (PKC) inhibitor bisindolylmaleimide 1 (Bis1) (500 nM), Src kinase inhibitor SU6656 (4 μM), MEK1/2 inhibitor U0126 (500 nM), RET inhibitor RPI-1 (50 μM), phosphatidylinositol-3-kinase (PI3K) inhibitors wortmannin (Wort.) (750 nM) or PIK-90 (750 nM), or mammalian target of rapamycin (mTOR) inhibitor rapamycin (Rapa.) (750 nM). The inhibitors were added 1 hour before GDNF and were present throughout the incubation. $A\beta_{1-40}$ data are shown relative to the G− control. Data are mean ± standard error of the mean ($n = 4$). * $p < 0.05$, ** $p < 0.01$. (B) Lysates were prepared from d9 LUHMES cells and analyzed by Western blot for the amounts of AKT and phosphorylated AKT (P-AKT). Cells had been treated as in (A) with GDNF plus inhibitors. For reference, samples from cells, grown for 9 days in G− or G+ medium, were loaded. GAPDH served as loading control. Two representative blots are displayed. (C) Quantification of P-AKT/AKT band intensity ratios from 3 experiments. "N.S." above the G+ bar refers to no statistically significant difference in comparison with G− + 2 ng/mL GDNF and DMSO/Rapa.

proteins. This was associated with increased secretase activities and resulted in rising Aβ_{1-40} levels. Our findings parallel observations in other neuronal cell lines that release Aβ preferentially in the differentiated, but not in the precursor state (Muresan and Muresan, 2006; Wertkin et al., 1993). During the early differentiation phase of LUHMES, *RET* was expressed at a constant level which was not affected by GDNF, and also Aβ_{1-40} generation was independent of GDNF-mediated signals. This is consistent with our findings that G− cells produced as much Aβ as G+ cells, and that RET knockdown did not have any effect on Aβ levels in d5 cells. The later maturation and aging stage of LUHMES was characterized by an increased release of Aβ and sAPPβ, although most AD-associated genes/proteins remained at constant levels. This late increase in Aβ is in accordance with the augmented Aβ production and the associated higher β-secretase activity observed in aging animals and humans (Fukumoto et al., 1996, 2004).

Before we further investigated the reasons for the Aβ rise in older cultures, we undertook a basic characterization of LUHMES as a new model to study wild type human APP processing. Pharmacological inhibition of β- or γ-secretase showed quantitative responses similar to the ones known for other cell models (Volbracht et al., 2009). Moreover, the alteration of amyloidogenic APP processing in LUHMES due to indirect modulation of secretases by cholesterol depletion was in line with the data from other cell and animal models (Fassbender et al., 2001; Guardia-Laguarta et al., 2009; Simons et al., 1998). These results demonstrate that the essential components for the proteolysis of APP and the regulation thereof are expressed in LUHMES. Interestingly, this machinery matured and relocalized during the initial days of differentiation. From d0–d2, the cells expressed the immature forms of APP and BACE, which are known to reside primarily in endoplasmic reticulum compartments. After d4, higher amounts of the mature neuronal forms of APP and BACE were detected, and this was associated with increasing amounts of cleavage products. Such maturation and interaction of APP and BACE are known to occur during trafficking through the Golgi to the cell surface and in the endocytic pathway (Zhang et al., 2011). Thus, we conclude that proteins in LUHMES undergo complete post-translational modification only after a certain progress of cell differentiation, reflecting the transition from a precursor to a typical neuronal phenotype. We also investigated whether Aβ_{1-42} was generated in parallel to Aβ_{1-40}, but we found that concentrations of Aβ_{1-42} in both the cell culture supernatants and the cell lysates were too low for detection by ELISA or Western blot analysis. This is most likely explained by the fact that cleavage of wild type APP by nonmutant γ-secretase generates preferentially Aβ_{1-40} and only approximately 5%–10% Aβ_{1-42} relative to total secreted Aβ peptides (Selkoe, 2002).

As second AD-relevant cell feature, we examined tau expression and modification, because it has been proposed that Aβ and tau pathologies are interactive (Roberson et al., 2007; Zheng et al., 2002). We detected an increase in phosphorylation of different tau isoforms during differentiation, in parallel to rising Aβ levels. Moreover, we observed a change of expression pattern of tau isoforms, which resembled the one observed in developing brain and in differentiating primary neurons in vitro (Buée et al., 2000; Deshpande et al., 2008). However, our results also showed that the Aβ increase was not functionally linked to increasing tau phosphorylation or vice versa.

We used the new model of APP processing to study the late increase of Aβ in aging LUHMES neurons. The major finding of this study is the regulation exerted by the GDNF-RET system. In fully differentiated LUHMES neurons, Aβ was induced by the presence of GDNF. This effect was reversible upon withdrawal of the growth factor and was also triggered by the related peptide NRTN. The 2 neurotrophic factors activate RET signaling (Buj-Bello et al., 1997; Trupp et al., 1996), leading to an upregulation of RET itself, likely via a positive feedback loop, as has been previously shown in a neuroblastoma cell line (Peterson and Bogenmann, 2004). We observed the same effect in LUHMES cells, and additionally, we saw that the abrogation of this feedback, i.e., the withdrawal of GDNF, resulted in an immediate downregulation of *RET* mRNA. Also NGF, which is not a RET ligand, triggered an Aβ increase. This may be based on a tyrosine kinase cross-signaling between TrkA and RET, which is well established for NGF, but not for related factors such as BDNF (Tsui-Pierchala et al., 2002). Most likely, canonical TrkA signaling without RET involvement is not responsible for the Aβ increase in LUHMES, as such effects are not observed in other cells expressing this receptor and releasing Aβ. On the contrary, rather a reverse correlation has been described for PC12 and hippocampal cells (Matrone et al., 2008b, 2009). Finally, we confirmed the involvement of RET in the GDNF-stimulated Aβ increase both by knockdown and by the use of a RET kinase inhibitor.

As downstream target of RET signaling, we identified here the PI3K pathway, because the PI3K inhibitors efficiently blocked the GDNF-triggered Aβ increase by G− cells, and also significantly reduced the amount of Aβ released by G+ cells. However, identification of the more proximal regulators of APP processing will require further investigation. It is remarkable that, besides *RET*, none of 88 AD-related genes showed differential expression in G− and G+ cells. This finding suggests that changes may only occur on the level of proteins. For instance, γ-secretase-activating protein may be involved (He et al., 2010), and posttranslational modifications of regulatory factors are likely to contribute to this. In this context, casein kinases and glycogen synthase kinase-3α (Flajolet et al., 2007; Phiel et al., 2003) have been shown to affect the generation of Aβ, and both APP and BACE are phosphorylated in the course of maturation (Oishi et al., 1997; Walter et al., 2001). Our

observation of altered AKT phosphorylation is in agreement with such direct regulation processes. However, we cannot rule out that GDNF also had indirect effects by altering degradation pathways of APP fragments. The mTOR pathway has been implicated in APP turnover (Spilman et al., 2010; Tian et al., 2011), and because inhibition of mTOR by rapamycin efficiently blocked the GDNF-stimulated Aβ increase in our experiments, our future investigations will focus on the role of autophagy. Our suggestion of a role of the PI3K pathway in the enhanced Aβ generation is well in line with some recent work (e.g., Stöhr et al., 2011), but others favor more the involvement of Src kinase (e.g., Minopoli et al., 2007). Possibly, the relative contribution of different pathways depends on the experimental system. For instance, the latter work used RET overexpression as a model for altered signaling events. This may replicate a situation of very high RET expression and availability of high concentrations of RET ligands. In such a situation, we would probably not find increased Aβ in our model, either. Furthermore, Minopoli et al. (2007) investigated mainly the generation of the intracellular C-terminal stub of APP, which we did not examine. This may well be dependent on other kinases than PI3K. Thus, we believe that there is no inconsistency between previous studies such as the one mentioned and our findings. However, different situations may require different biochemical explanations. This is nicely demonstrated by our data showing the differences between d5 cells (Aβ generation independent of PI3K, also in the presence of GDNF) and d9 cells (Aβ generation dependent on RET activation).

Our findings, that the stimulation of Aβ release from G− cells reaches a maximum at 2 ng/mL GDNF or 20 ng/mL NRTN, points at a negative feedback loop that predominates at high receptor occupancy. One of the underlying mechanisms may be the removal of RET from the cell surface. It is known that RET, either alone or in complex with GFLs, can be internalized and degraded in proteasomes after ligand-induced activation (Pierchala et al., 2006; Scott et al., 2005). The realistic GDNF concentrations to be expected in brain are rather in the ascending part of the bell-shaped curve of Aβ increase, also when increased concentrations under pathological conditions are considered. Such increases are supported by a recent study that revealed raised levels of GDNF in cerebrospinal fluid of AD patients (Straten et al., 2009).

One interesting finding in this context was that also sAPPα generation was strongly dependent on the GDNF concentration. While it clearly decreased at "optimal" (Aβ-increasing) concentrations, this decrease was absent at high GDNF concentrations. Moreover, prolonged stimulation of cells with GDNF (as in G+ cells) resulted in no significant sAPPα reduction in G+ cells compared with G− cells. Therefore, the sAPPα effect may be a rather temporary and secondary response, although we cannot exclude that small sAPPα alterations were simply not detectable (due to the ELISA sensitivity), as was the case for sAPPβ in the GDNF stimulation experiments.

Although neurotrophic signaling is generally regarded as positive for the brain, and several growth factors promote the nonamyloidogenic processing of APP by α-secretase (Adlerz et al., 2007; Matrone et al., 2008a; Rossner et al., 1998), we revealed here a possibly detrimental side effect of raised GDNF levels. Epidermal growth factor, NGF, and platelet-derived growth factor have also been shown to enhance amyloidogenic processing of APP (Gianni et al., 2003; Zou et al., 2007). Moreover, NGF was reported to strongly increase the neurotoxic potency of Aβ (Yankner et al., 1990). Midbrain neurons, which express GDNF receptors, have been shown to generate Aβ (Cai et al., 2010) and may contribute to disease pathogenesis (Muresan and Muresan, 2008). For instance, nigral neurodegeneration and Aβ plaques in the striatum are observed in AD patients (Uchihara et al., 1992; Villemagne et al., 2009). Our study provides some mechanistic rationale for these findings and suggests further investigation. This might be particularly relevant for cases of combined AD and Parkinson's disease pathologies (Kalaitzakis and Pearce, 2009; Kalaitzakis et al., 2008) and when GDNF treatment is considered as a therapeutic approach for Parkinson's disease.

Disclosure statement

The authors declare no conflict of interest.

Acknowledgements

We thank many colleagues, especially B. Zimmer, for helpful advice and valuable discussions. We acknowledge Dr. Joachim Hentschel from the Electron Microscope Service Facility for technical assistance. The work was supported by grants from the Doerenkamp-Zbinden foundation, the Land Baden-Württemberg and the DFG. D.S. was funded by an IRTG1331 fellowship.

References

Adlerz, L., Holback, S., Multhaup, G., Iverfeldt, K., 2007. IGF-1-induced processing of the amyloid precursor protein family is mediated by different signaling pathways. J. Biol. Chem. 282, 10203–10209.

Airaksinen, M.S., Saarma, M., 2002. The GDNF family: signalling, biological functions and therapeutic value. Nat. Rev. Neurosci. 3, 383–394.

Ballatore, C., Lee, V.M., Trojanowski, J.Q., 2007. Tau-mediated neurodegeneration in Alzheimer's disease and related disorders. Nat. Rev. Neurosci. 8, 663–672.

Baxter, E.W., Conway, K.A., Kennis, L., Bischoff, F., Mercken, M.H., Winter, H.L., Reynolds, C.H., Tounge, B.A., Luo, C., Scott, M.K.,

Huang, Y., Braeken, M., Pieters, S.M., Berthelot, D.J., Masure, S., Bruinzeel, W.D., Jordan, A.D., Parker, M.H., Boyd, R.E., Qu, J., Alexander, R.S., Brenneman, D.E., Reitz, A.B., 2007. 2-Amino-3,4-dihydroquinazolines as inhibitors of BACE-1 (beta-site APP cleaving enzyme): use of structure based design to convert a micromolar hit into a nanomolar lead. J. Med. Chem. 50, 4261–4264.

Buée, L., Bussière, T., Buée-Scherrer, V., Delacourte, A., Hof, P.R., 2000. Tau protein isoforms, phosphorylation and role in neurodegenerative disorders. Brain Res. Brain Res. Rev. 33, 95–130.

Buj-Bello, A., Adu, J., Piñón, L.G., Horton, A., Thompson, J., Rosenthal, A., Chinchetru, M., Buchman, V.L., Davies, A.M., 1997. Neurturin responsiveness requires a GPI-linked receptor and the Ret receptor tyrosine kinase. Nature 387, 721–724.

Cai, Y., Xiong, K., Zhang, X.M., Cai, H., Luo, X.G., Feng, J.C., Clough, R.W., Struble, R.G., Patrylo, P.R., Chu, Y., Kordower, J.H., Yan, X.X., 2010. β-Secretase-1 elevation in aged monkey and Alzheimer's disease human cerebral cortex occurs around the vasculature in partnership with multisystem axon terminal pathogenesis and β-amyloid accumulation. Eur. J. Neurosci. 32, 1223–1238.

Cuccuru, G., Lanzi, C., Cassinelli, G., Pratesi, G., Tortoreto, M., Petrangolini, G., Seregni, E., Martinetti, A., Laccabue, D., Zanchi, C., Zunino, F., 2004. Cellular effects and antitumor activity of RET inhibitor RPI-1 on MEN2A-associated medullary thyroid carcinoma. J. Natl. Cancer Inst. 96, 1006–1014.

Deshpande, A., Win, K.M., Busciglio, J., 2008. Tau isoform expression and regulation in human cortical neurons. FASEB J. 22, 2357–2367.

Falsig, J., Latta, M., Leist, M., 2004. Defined inflammatory states in astrocyte cultures: correlation with susceptibility towards CD95-driven apoptosis. J. Neurochem. 88, 181–193.

Fassbender, K., Simons, M., Bergmann, C., Stroick, M., Lutjohann, D., Keller, P., Runz, H., Kuhl, S., Bertsch, T., von Bergmann, K., Hennerici, M., Beyreuther, K., Hartmann, T., 2001. Simvastatin strongly reduces levels of Alzheimer's disease beta -amyloid peptides Abeta 42 and Abeta 40 in vitro and in vivo. Proc. Natl. Acad. Sci. U. S. A. 98, 5856–5861.

Flajolet, M., He, G., Heiman, M., Lin, A., Nairn, A.C., Greengard, P., 2007. Regulation of Alzheimer's disease amyloid-beta formation by casein kinase I. Proc. Natl. Acad. Sci. U. S. A. 104, 4159–4164.

Fukumoto, H., Asami-Odaka, A., Suzuki, N., Shimada, H., Ihara, Y., Iwatsubo, T., 1996. Amyloid beta protein deposition in normal aging has the same characteristics as that in Alzheimer's disease. Predominance of A beta 42(43) and association of A beta 40 with cored plaques. Am. J. Pathol. 148, 259–265.

Fukumoto, H., Rosene, D.L., Moss, M.B., Raju, S., Hyman, B.T., Irizarry, M.C., 2004. Beta-secretase activity increases with aging in human, monkey, and mouse brain. Am. J. Pathol. 164, 719–725.

Futami, H., Sakai, R., 2009. RET protein promotes non-adherent growth of NB-39-nu neuroblastoma cell line. Cancer Sci. 100, 1034–1039.

Gianni, D., Zambrano, N., Bimonte, M., Minopoli, G., Mercken, L., Talamo, F., Scaloni, A., Russo, T., 2003. Platelet-derived growth factor induces the beta-gamma-secretase-mediated cleavage of Alzheimer's amyloid precursor protein through a Src-Rac-dependent pathway. J. Biol. Chem. 278, 9290–9297.

Gosh, A.K., Shin, D., Downs, D., Koelsch, G., Lin, X., Ermolieff, J., Tang, J., 2000. Design of potent inhibitors for human brain memapsin 2 (β-secretase). J. Am. Chem. Soc. 122, 3522–3523.

Guardia-Laguarta, C., Coma, M., Pera, M., Clarimón, J., Sereno, L., Agulló, J.M., Molina-Porcel, L., Gallardo, E., Deng, A., Berezovska, O., Hyman, B.T., Blesa, R., Gómez-Isla, T., Lleó, A., 2009. Mild cholesterol depletion reduces amyloid-beta production by impairing APP trafficking to the cell surface. J. Neurochem. 110, 220–230.

He, G., Luo, W., Li, P., Remmers, C., Netzer, W.J., Hendrick, J., Bettayeb, K., Flajolet, M., Gorelick, F., Wennogle, L.P., Greengard, P., 2010. Gamma-secretase activating protein is a therapeutic target for Alzheimer's disease. Nature 467, 95–98.

Hsiao, K., Chapman, P., Nilsen, S., Eckman, C., Harigaya, Y., Younkin, S., Yang, F., Cole, G., 1996. Correlative memory deficits, Abeta elevation, and amyloid plaques in transgenic mice. Science 274, 99–102.

Ittner, L.M., Götz, J., 2011. Amyloid-beta and tau—a toxic pas de deux in Alzheimer's disease. Nat. Rev. Neurosci. 12, 65–72.

Kalaitzakis, M.E., Graeber, M.B., Gentleman, S.M., Pearce, R.K., 2008. Striatal beta-amyloid deposition in Parkinson disease with dementia. J. Neuropathol. Exp. Neurol. 67, 155–161.

Kalaitzakis, M.E., Pearce, R.K., 2009. The morbid anatomy of dementia in Parkinson's disease. Acta Neuropathol. 118, 587–598.

Karreman, C., 2002. AiO, combining DNA/protein programs and oligomanagement. Bioinformatics 18, 884–885.

Lotharius, J., Barg, S., Wiekop, P., Lundberg, C., Raymon, H.K., Brundin, P., 2002. Effect of mutant alpha-synuclein on dopamine homeostasis in a new human mesencephalic cell line. J. Biol. Chem. 277, 38884–38894.

Lotharius, J., Falsig, J., van Beek, J., Payne, S., Dringen, R., Brundin, P., Leist, M., 2005. Progressive degeneration of human mesencephalic neuron-derived cells triggered by dopamine-dependent oxidative stress is dependent on the mixed-lineage kinase pathway. J. Neurosci. 25, 6329–6342.

Manié, S., Santoro, M., Fusco, A., Billaud, M., 2001. The RET receptor: function in development and dysfunction in congenital malformation. Trends Genet. 17, 580–589.

Matrone, C., Ciotti, M.T., Mercanti, D., Marolda, R., Calissano, P., 2008a. NGF and BDNF signaling control amyloidogenic route and Abeta production in hippocampal neurons. Proc. Natl. Acad. Sci. U. S. A. 105, 13139–13144.

Matrone, C., Di Luzio, A., Meli, G., D'Aguanno, S., Severini, C., Ciotti, M.T., Cattaneo, A., Calissano, P., 2008b. Activation of the amyloidogenic route by NGF deprivation induces apoptotic death in PC12 cells. J. Alzheimers Dis. 13, 81–96.

Matrone, C., Marolda, R., Ciafrè, S., Ciotti, M.T., Mercanti, D., Calissano, P., 2009. Tyrosine kinase nerve growth factor receptor switches from prosurvival to proapoptotic activity via Abeta-mediated phosphorylation. Proc. Natl. Acad. Sci. U. S. A. 106, 11358–11363.

Minopoli, G., Passaro, F., Aloia, L., Carlomagno, F., Melillo, R.M., Santoro, M., Forzati, F., Zambrano, N., Russo, T., 2007. Receptor- and non-receptor tyrosine kinases induce processing of the amyloid precursor protein: role of the low-density lipoprotein receptor-related protein. Neurodegener. Dis. 4, 94–100.

Muresan, Z., Muresan, V., 2006. Neuritic deposits of amyloid-beta peptide in a subpopulation of central nervous system-derived neuronal cells. Mol. Cell. Biol. 26, 4982–4997.

Muresan, Z., Muresan, V., 2008. Seeding neuritic plaques from the distance: a possible role for brainstem neurons in the development of Alzheimer's disease pathology. Neurodegener. Dis. 5, 250–253.

Oishi, M., Nairn, A.C., Czernik, A.J., Lim, G.S., Isohara, T., Gandy, S.E., Greengard, P., Suzuki, T., 1997. The cytoplasmic domain of Alzheimer's amyloid precursor protein is phosphorylated at Thr654, Ser655, and Thr668 in adult rat brain and cultured cells. Mol. Med. 3, 111–123.

Peterson, S., Bogenmann, E., 2004. The RET and TRKA pathways collaborate to regulate neuroblastoma differentiation. Oncogene 23, 213–225.

Phiel, C.J., Wilson, C.A., Lee, V.M., Klein, P.S., 2003. GSK-3alpha regulates production of Alzheimer's disease amyloid-beta peptides. Nature 423, 435–439.

Pierchala, B.A., Milbrandt, J., Johnson, E.M., Jr., 2006. Glial cell line-derived neurotrophic factor-dependent recruitment of Ret into lipid rafts enhances signaling by partitioning Ret from proteasome-dependent degradation. J. Neurosci. 26, 2777–2787.

Roberson, E.D., Scearce-Levie, K., Palop, J.J., Yan, F., Cheng, I.H., Wu, T., Gerstein, H., Yu, G.Q., Mucke, L., 2007. Reducing endogenous tau ameliorates amyloid beta-induced deficits in an Alzheimer's disease mouse model. Science 316, 750–754.

Rossner, S., Ueberham, U., Schliebs, R., Perez-Polo, J.R., Bigl, V., 1998. The regulation of amyloid precursor protein metabolism by cholinergic mechanisms and neurotrophin receptor signaling. Prog. Neurobiol. 56, 541–569.

Sadeghi, M.M., Collinge, M., Pardi, R., Bender, J.R., 2000. Simvastatin modulates cytokine-mediated endothelial cell adhesion molecule induction: involvement of an inhibitory G protein. J. Immunol. 165, 2712–2718.

Schildknecht, S., Pape, R., Müller, N., Robotta, M., Marquardt, A., Bürkle, A., Drescher, M., Leist, M., 2011. Neuroprotection by minocycline caused by direct and specific scavenging of peroxynitrite. J. Biol. Chem. 286, 4991–5002.

Schildknecht, S., Pöltl, D., Nagel, D.M., Matt, F., Scholz, D., Lotharius, J., Schmieg, N., Salvo-Vargas, A., Leist, M., 2009. Requirement of a dopaminergic neuronal phenotype for toxicity of low concentrations of 1-methyl-4-phenylpyridinium to human cells. Toxicol. Appl. Pharmacol. 241, 23–35.

Scholz, D., Pöltl, D., Genewsky, A., Weng, M., Waldmann, T., Schildknecht, S., Leist, M., 2011. Rapid, complete and large-scale generation of post-mitotic neurons from the human LUHMES cell line. J. Neurochem. 119, 957–971.

Scott, R.P., Eketjäll, S., Aineskog, H., Ibáñez, C.F., 2005. Distinct turnover of alternatively spliced isoforms of the RET kinase receptor mediated by differential recruitment of the Cbl ubiquitin ligase. J. Biol. Chem. 280, 13442–13449.

Selkoe, D.J., 2002. Deciphering the genesis and fate of amyloid beta-protein yields novel therapies for Alzheimer disease. J. Clin. Invest. 110, 1375–1381.

Simons, M., Keller, P., De Strooper, B., Beyreuther, K., Dotti, C.G., Simons, K., 1998. Cholesterol depletion inhibits the generation of beta-amyloid in hippocampal neurons. Proc. Natl. Acad. Sci. U. S. A. 95, 6460–6464.

Spilman, P., Podlutskaya, N., Hart, M.J., Debnath, J., Gorostiza, O., Bredesen, D., Richardson, A., Strong, R., Galvan, V., 2010. Inhibition of mTOR by rapamycin abolishes cognitive deficits and reduces amyloid-beta levels in a mouse model of Alzheimer's disease. PLoS One 5, e9979.

Stachel, S.J., Coburn, C.A., Steele, T.G., Jones, K.G., Loutzenhiser, E.F., Gregro, A.R., Rajapakse, H.A., Lai, M.T., Crouthamel, M.C., Xu, M., Tugusheva, K., Lineberger, J.E., Pietrak, B.L., Espeseth, A.S., Shi, X.P., Chen-Dodson, E., Holloway, M.K., Munshi, S., Simon, A.J., Kuo, L., Vacca, J.P., 2004. Structure-based design of potent and selective cell-permeable inhibitors of human beta-secretase (BACE-1). J. Med. Chem. 47, 6447–6450.

Stiegler, N.V., Krug, A.K., Matt, F., Leist, M., 2011. Assessment of chemical-induced impairment of human neurite outgrowth by multiparametric live cell imaging in high-density cultures. Toxicol. Sci. 121, 73–87.

Stöhr, O., Schilbach, K., Moll, L., Hettich, M.M., Freude, S., Wunderlich, F.T., Ernst, M., Zemva, J., Bruning, J.C., Krone, W., Udelhoven, M., Schubert, M., 2011. Insulin receptor signaling mediates APP processing and beta-amyloid accumulation without altering survival in a transgenic mouse model of Alzheimer's disease. Age [Dordr]. doi: 10.1007/s11357-011-9333-2.

Straten, G., Eschweiler, G.W., Maetzler, W., Laske, C., Leyhe, T., 2009. Glial cell-line derived neurotrophic factor (GDNF) concentrations in cerebrospinal fluid and serum of patients with early Alzheimer's disease and normal controls. J. Alzheimers Dis. 18, 331–337.

Takahashi, M., 2001. The GDNF/RET signaling pathway and human diseases. Cytokine Growth Factor Rev. 12, 361–373.

Tian, Y., Bustos, V., Flajolet, M., Greengard, P., 2011. A small-molecule enhancer of autophagy decreases levels of Abeta and APP-CTF via Atg5-dependent autophagy pathway. FASEB J. 25, 1934–1942.

Trupp, M., Arenas, E., Fainzilber, M., Nilsson, A.S., Sieber, B.A., Grigoriou, M., Kilkenny, C., Salazar-Grueso, E., Pachnis, V., Arumäe, U., 1996. Functional receptor for GDNF encoded by the c-ret proto-oncogene. Nature 381, 785–789.

Tsui-Pierchala, B.A., Milbrandt, J., Johnson, E.M., Jr., 2002. NGF utilizes c-Ret via a novel GFL-independent, inter-RTK signaling mechanism to maintain the trophic status of mature sympathetic neurons. Neuron 33, 261–273.

Uchihara, T., Kondo, H., Kosaka, K., Tsukagoshi, H., 1992. Selective loss of nigral neurons in Alzheimer's disease: a morphometric study. Acta Neuropathol. 83, 271–276.

Villemagne, V.L., Ataka, S., Mizuno, T., Brooks, W.S., Wada, Y., Kondo, M., Jones, G., Watanabe, Y., Mulligan, R., Nakagawa, M., Miki, T., Shimada, H., O'Keefe, G.J., Masters, C.L., Mori, H., Rowe, C.C., 2009. High striatal amyloid beta-peptide deposition across different autosomal Alzheimer disease mutation types. Arch. Neurol. 66, 1537–1544.

Volbracht, C., Penzkofer, S., Mansson, D., Christensen, K.V., Fog, K., Schildknecht, S., Leist, M., Nielsen, J., 2009. Measurement of cellular beta-site of APP cleaving enzyme 1 activity and its modulation in neuronal assay systems. Anal. Biochem. 387, 208–220.

Walter, J., Fluhrer, R., Hartung, B., Willem, M., Kaether, C., Capell, A., Lammich, S., Multhaup, G., Haass, C., 2001. Phosphorylation regulates intracellular trafficking of beta-secretase. J. Biol. Chem. 276, 14634–14641.

Wells, S.A., Jr., Santoro, M., 2009. Targeting the RET pathway in thyroid cancer. Clin. Cancer Res. 15, 7119–7123.

Wertkin, A.M., Turner, R.S., Pleasure, S.J., Golde, T.E., Younkin, S.G., Trojanowski, J.Q., Lee, V.M., 1993. Human neurons derived from a teratocarcinoma cell line express solely the 695-amino acid amyloid precursor protein and produce intracellular beta-amyloid or A4 peptides. Proc. Natl. Acad. Sci. U. S. A. 90, 9513–9517.

Yankner, B.A., Caceres, A., Duffy, L.K., 1990. Nerve growth factor potentiates the neurotoxicity of beta amyloid. Proc. Natl. Acad. Sci. U. S. A. 87, 9020–9023.

Zhang, Y.W., Thompson, R., Zhang, H., Xu, H., 2011. APP processing in Alzheimer's disease. Mol Brain 4, 3.

Zheng, W.H., Bastianetto, S., Mennicken, F., Ma, W., Kar, S., 2002. Amyloid beta peptide induces tau phosphorylation and loss of cholinergic neurons in rat primary septal cultures. Neuroscience 115, 201–211.

Zou, L., Wang, Z., Shen, L., Bao, G.B., Wang, T., Kang, J.H., Pei, G., 2007. Receptor tyrosine kinases positively regulate BACE activity and Amyloid-beta production through enhancing BACE internalization. Cell Res. 17, 389–401.